The numerical tool for a posteriori detection of boundary layers in *hp*-adaptive analysis

Łukasz Miazio[1] **and Grzegorz Zboinski**[1,2]

[1]*Faculty of Technical Sciences, University of Warmia and Mazury*
ul.Oczapowskiego 11; 10-719 Olsztyn, Poland
e-mail: lukasz.miazio@uwm.edu.pl

[2]*Institute of Fluid Flow Machinery, Polish Academy of Sciences*
ul. Fiszera 14, 80-952 Gdańsk, Poland
e-mail: zboi@imp.gda.pl

Abstract

The presented paper concerns *a posteriori* detection of the boundary layers in thin or thick elastic structures analyzed by means of the *hp*-adaptive finite element methods (FEM). In the paper we recall some analytical considerations concerning boundary layers theory. Then we present the idea of our detection tool based on the element residual method (ERM) of error estimation. The method of detection is based on solution of three local (element) problems defined analogously to ERM local problems. The first problem is solved for a boundary couple of two undivided triangular-prism elements. In the second and third problems the two-element mesh is divided by two uniformly and exponentially towards the boundary. This way two four-element local problems are formed. The corresponding solutions are compared with the solution of the first local problem. Finally, we check numerically effectiveness of our detection method for the meshes of varying density applied to the model plate problem.

Keywords: plates, finite element methods, adaptivity, error estimation, numerical analysis

1. Introduction

1.1. General remarks

The boundary layer effect appears in the case of the thin or thick-walled structures. The analytical explanation of this effect is presented in the numerous papers and text books (see [1, 2], for example). In most cases of such structures, the solution is composed of the smooth part in the internal zone of the structure and the part of high solution gradients in the boundary zones. In the numerical implementations, the problem solution needs application of the solution spaces rich enough to reflect high solution gradients in the vicinity of the boundaries. The most common method of space enrichment lies in application of the mesh refined exponentially in the direction normal to the boundary. Numerous papers address the issue (see [3, 4], for example). Note that such space enrichment is both numerically complex and costly due to application of the non-uniform mesh subdivisions and different treatment of the internal and boundary zones of the structure. However, without the space enrichment the solution convergence can be affected seriously.

1.2. Objective of our research

The presented paper is a part of the general research on *hp*-adaptive static and dynamic analysis of complex structures composed of thin-walled, thick-walled and solid parts. We search for a quite general numerical tool for adaptive modeling and analysis of wide variety of problems within solid mechanics. In this approach we apply: hierarchical modeling, hierarchical *hp*-approximations, element residual equilibration method of error estimation, and error-controlled *hp*-adaptivity.

In this paper we address the problem of automatic numerical resolution of the boundary layers, suitable for the standard *hp*-adaptive approach. In particular, we search for a numerical tool for detection, and possibly range and intensity assessment, of the boundary layers. With this tool at hand, we do hope to be able to *h*-refine our initial mesh towards the boundaries exponentially so as to obtain the modified mesh capable of resolution of the boundary layers via standard two-step *hp*-approach.

The starting point for the research are the results of our previous efforts described in [6, 8]. The results of these efforts have been quite promising, yet not totally satisfactory, especially in terms of general applicability of the previously proposed approach.

The main objective of this paper is to present the enhanced general numerical tool for detection of the boundary layers a posteriori and to assess its effectiveness. Note that the authors of this papers are not aware of any alternative general tools for such detection.

2. A posteriori boundary layer detection

2.1. The boundary layer phenomenon

It should be stated first that In the case of Kirchhoff plates the boundary layer phenomena do not appear [6]. It results from the fact that the problem is described with a biharmonic equilibrium equation. The solution to such an equation is always smooth, regardless of the applied boundary conditions. In our further considerations, however, we will address the case of Reisner-Mindlin plates, the equilibrium of which is described with the relations derived in work [5]

$$\frac{D}{2}\left[(1-\nu)\left(\partial_1^2\theta_n+\partial_2^2\theta_n\right)+(1-\nu)\left(\partial_1\partial_n\theta_1+\partial_2\partial_n\theta_2\right)\right]+ \\ +\frac{Et}{2(1+\nu)}\left(\theta_n-\partial_n u_3\right)=0, \tag{1}$$

$$\frac{Et}{2(1-\nu)}\left(\partial_1\theta_1+\partial_2\theta_2-\partial_1^2 u_3-\partial_2^2 u_3\right)=q(x_1,x_2), \tag{2}$$

where:
θ_n, n = 1, 2 – rotation angles of the shell mid-surface,
u_3 – plate deflection,
1, 2, 3 – the indices denoting two longitudinal and third transverse directions of the global Cartesian system of coordinates,
D – an auxiliary variable, defined as in the case of the first order plate theory,
i.e. $D = \frac{Et^3}{12(1-\nu^2)}$,
$q = q(x_1,x_2)$ – stands for the transverse (normal) traction of the plate.

It is worth noticing that diferentiation of two relations (1) with respect to two n directions (n = 1, 2) and their substitution into the left-hand side sum of (2), leads to the biharmonic equations of the form (compare [6]):

$$\partial_1^4 u_3 + 2\partial_1^4\partial_2^4 u_3 + \partial_2^4 u_3 = \frac{q}{D} - \frac{1+\nu}{Et}\left(\partial_1^2 q + \partial_2^2 q\right). \tag{3}$$

It can be concluded then, that the solution defining the deflection of the Reissner-Mindlin plate is smooth, similarly to the Kirchhoff plate solution [6].

The smooth character of the function u_3 seems to be clear. On the contrary, the solutions for rotations θ_n, n = 1,2 do not necessarily possess this feature. In view of this, we will assume

$$u_3(x_1,x_2) = u_3^G(x_1,x_2), \tag{4}$$

$$\theta_n(x_1,x_2) = \theta_n^G(x_1,x_2) + \theta_n^B(x_1,x_2),\ n = 1,2, \tag{5}$$

where:
G – notion of the smooth part of the solution,
B – notion of the boundary part of the solution.

The smooth solution for the transverse displacement $u_3^G(x_1,x_2)$ can now be obtained directly, substitiuting (4) into (3). This solution can now be associated with the equation (1), in which we assume $\theta_n(x_1,x_2) \equiv \theta_n^G(x_1,x_2), n = 1,2$. This allows to determine the smooth part of the rotations. Determination of the boundary part of the transverse displacements is not necessary, as $u_3^B(x_1,x_2) \equiv 0$. Taking this into account, one may write equations (1) and (2) in the simplified form

$$\frac{D}{2}(1-\nu)\left(\partial_1^2\theta_n + \partial_2^2\theta_n\right) + \frac{Et}{2(1+\nu)}\theta_n = 0,\ n = 1,2, \tag{6}$$

$$\frac{Et}{2(1+\nu)}\left(\partial_1\theta_1 + \partial_2\theta_2\right) = 0, \tag{7}$$

where (7) has been substituted into (6). The above relations, after assuming that $\theta_n(x_1,x_2) = \theta_n^B(x_1,x_2)$, allow for determination of the boundary part of the rotations, $\theta_n^B(x_1,x_2)$.

Basing on the above considerations one can find the solution for plates, subject to boundary layer phenomenon, of an infinite length in the direction of x_1 and the width a in the direction x_2. This is done in the works [4, 8, 24]. The approach presented in these works is based on the perturbation method and the assumption of a solution in the form of asymptotic series

$$u_3(x_1,x_2) = \sum_{i=0}^{\infty} t^i u_{3,i}^G(x_1,x_2), \tag{8}$$

$$\theta_n(x_1,x_2) = \sum_{i=0}^{\infty} t^i\left[\theta_{n,i}^G(x_1,x_2) + \theta_{n,i}^B(x_1,x_2)\right],\ n = 1,2, \tag{9}$$

where the consecutive terms representing the boundary part of the solution can be written as

$$\theta_{n,i}^B(x_1,x_2) = C_{n,i}(x_1)e^{-\gamma a\frac{x_2}{t}},\ n = 1,2 \tag{10}$$

and where:
t – the plate thickness.

In the above relation, the terms $C_{n,i}(x_1)$ and $e^{-\gamma a\frac{x_2}{t}}$ describe a smooth function in the direction tangential to the plate boundary and an exponentially decreasing function in the direction normal to this boundary, with γ standing for a constant dependant on the order of regularity of the solution. The boundary solutions for rotations include a different number of terms (10) in the series (8) and (9). The lower the order of the first term of the series, the greater the effect on the boundary solution [7]. It is the exponential function of (10) that makes it necessary to use fine meshes in the case of boundary layer phenomena.

2.2. The idea of the detection tool

The proposed method of detection of a boundary layer is related the method of our work [6]. The method takes advantage of the local (element) solutions, contributing to the upper bound of the exact solution, and obtained with the equilibrated residual method.

In order to detect the phenomenon we solve the local problem thrice within the domain V_c of a chosen couple of prismatic elements adjacent to the boundary S of a structure. The stresses $\langle \mathbf{r} \rangle$ on the internal boundary S_c of the chosen domain are known from the global solution obtained from the initial mesh. They equilibrate the external loading due to body and surface tractions, acting in V_c and on the supported Q and loaded P parts of the structure boundary. Firstly, we obtain the reference local solution on the two-element mesh based on the division pattern from the global problem. We choose two elements adjacent to the boundary and call them parent ones. The corresponding division numbers in the directions normal and tangent to the boundary are M_n = 1 and M_s = 1, respectively. Next we solve two four-element problems, applying algebraic and exponential divisions in the direction normal to the boundary (M_n = 2 and M_s = 1). The situation is illustrated in Fig. 1. The corresponding division ratios are denoted as ρ. This way we form two sub-domains f = 1, 2 with two prismatic elements in each sub-domain (i = 1,2). All the problems to be solved can be defined as follows

$$\sum_{f=1}^{2}\sum_{i=1}^{M_n}\left[B_{f_i}\left(\mathbf{u}_{f_i}^{HPQ}, \delta\mathbf{u}_{f_i}^{HPQ}\right) - L_{f_i}\left(\delta\mathbf{u}_{f_i}^{HPQ}\right) - \int_{S_c\cap S_{fi}/P\cup Q} \delta\mathbf{u}_{f_i}^{HPQ\,T}\left\langle \mathbf{r}_{f_i}\left(\mathbf{u}_{f_i}^{HPQ}\right)\right\rangle dS_{f_i}\right] = 0, \tag{11}$$

where: B stands for the bilinear form representing virtual strain energy, L is the virtual work of external forces, while $\boldsymbol{u}$ represents displacement vector. In the above equation H, P and Q represent element size, and its horizontal and vertical orders of approximation, all applied in the local problem.

While solving the second local problem (11), one has to determine local discretization parameters H, P and Q. Their values take advantage of the corresponding values of h, p, and q from the global problem. The local values of the parameters

have to correspond to boundary layer appearance, without numerical locking present. Taking this into account, we assume $H \equiv H_1 \equiv (H_{n_1}, H_{s_1})$, $H_{s_1} = h$, $H_{n_1} = H_{n_{art}}$, $P \equiv P_1 = P_{\max} \geq 8$, $Q \equiv Q_1 = q$.

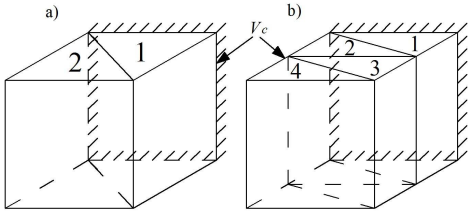

Figure 1: A boundary pair of parent elements (a) and four elements obtained by subdivision (b)

In the third local problem the mesh dimensions are set so as the boundary layer effect does not appear. This means that the following relations hold: $H_2 \equiv (H_{n_2}, H_{s_2})$, $H_{s_2} = H_{s_1} = h$, $H_{n_2} = H_{n_{\exp}}$, $P \equiv P_2 = P_1 = P_{\max} \geq 8$, $Q \equiv Q_2 = Q_1 = q$.

Above, the sizes $H_{n_{\exp}}$ and $H_{n_{art}}$ correspond to exponential and arithmetic subdivision by two of a parent pair of elements in the direction normal to the boundary, i.e. $M_n \equiv M_{n_{\exp}} = M_{n_{art}} = 2$. In this situation we have: $H_{n_{art}} = h/2$, $H_{n_{\exp}} = 9h/10$ with $f = 2$ corresponding to the boundary-adjacent pair of elements.

Let us introduce now a condition based on estimates U_4 of the strain energy corresponding to two above four-element local problems [6]

$$\sum_{f=1}^{2}\sum_{i=1}^{M_n}\frac{1}{2}B_{f_i}\left(u_{f_i}^{H_1P_1Q_1}, u_{f_i}^{H_1P_1Q_1}\right) < \sum_{f=1}^{2}\sum_{i=1}^{M_n}\frac{1}{2}B_{f_i}\left(u_{f_i}^{H_2P_1Q_1}, u_{f_i}^{H_2P_1Q_1}\right). \qquad (12)$$

Fulfillment or not of the above condition leads to the conclusion that the boundary layer phenomenon occurs or not, respectively.

Our element method of detection of the edge effects can be applied to each finite element pair, adjacent to the concerned boundary segment. In practice, it appears enough, however, to check the condition (12) for the selected pairs of finite elements along the boundary segment.

2.3. The detection criterion

The proposed criterion takes advantage of the condition (12). The criterion is based on comparison of the relative values of the differences between the strain energies, U_2 and U_4, obtained from the two- and four-element local problems, respectively. We calculate two such differences. One is based on the four-element mesh refined arithmetically and the other one on the exponentially divided mesh. If the solution from the exponential mesh is better, i.e. the value of the corresponding strain energy is higher, then the boundary effect may play a significant role. In the opposite case the boundary layer effect is negligible.

3. Numerical experiments

Our calculations are performed for a model plate problem. Due to the symmetry we analyze a quarter of the square plate. The plate length is l = 1,57075·10^{-2} [m], while its thickness is equal to t = 0,03·10^{-2}. The Young modulus is E=2,11·10^{11} [N/m^2] and the Poisson's ratio equals 0.3. The plate is loaded with uniform normal traction p = -4,0·10^6 [N/m^2] and clamped around its lateral boundaries. We apply two 3D-based mechanical models of the plate: the hierarchical shell model of the transverse order q = 2 and the Reissner-Mindlin plate model (q = 1).

In our numerical tests we utilize regular 3x3, 4x4 and 8x8 meshes displayed in Figs 2, 3 and 4, respectively. The respective numbering of elements is also presented in these figures.

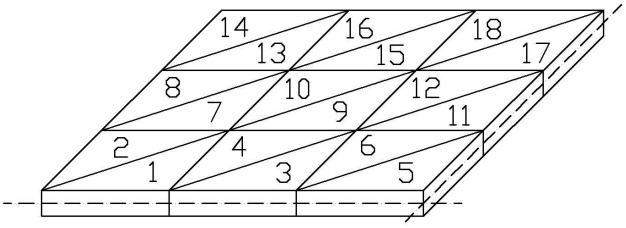

Figure 2: The global numbering of elements (3x3 regular mesh)

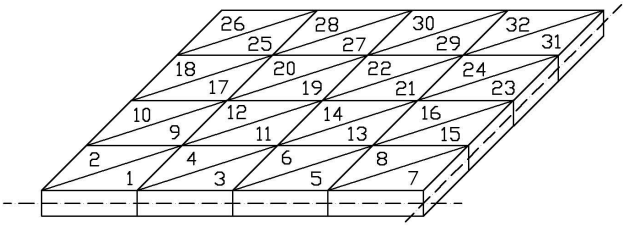

Figure 3: The global numbering of elements (4x4 regular mesh)

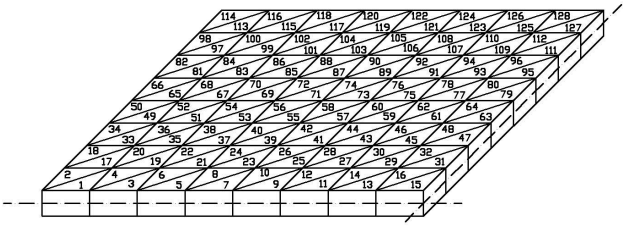

Figure 4: The global numbering of elements of the 8x8 mesh

In order to detect the boundary layer and to assess its influence on the solution we perform a kind of sensitivity analysis. We change the division ratio ρ in the four-element local problem and refer the corresponding value of the strain energy to its value obtained from the two-element local problem, i.e.

$$\eta_{\%} = \frac{|U_4 - U_2|}{U_2} \cdot 100\% . \qquad (13)$$

The results of our analysis are shown in Figs. 5 to 10, where the values of $\eta_{\%}$ are displayed as a function of the division ratio. The value of the ratio equal to 1 corresponds to the uniform (algebraic) division, while the value of 10 says that two elements adjacent to the boundary are ten times narrower than the other pair of elements resulting from the division. Each of the presented curves is marked with the numbers of two corresponding parent elements chosen out of the elements displayed in Figs 2, 3 and 4.

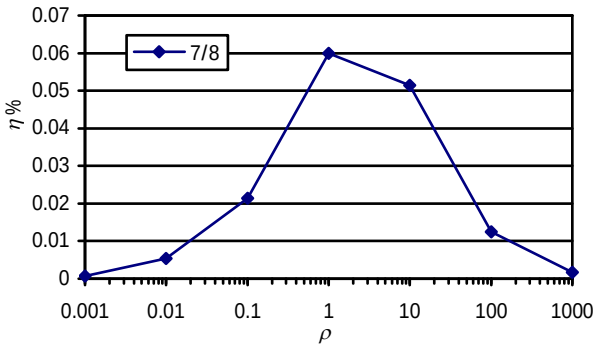

Figure 5: Local problem results (Reissner-Mindlin plate model, 3x3 mesh)

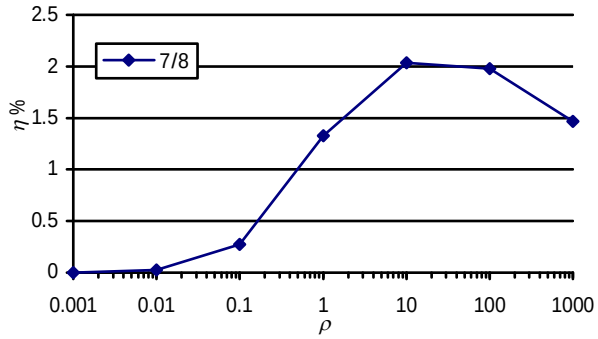

Figure 6: Local problem results (hierarchical plate model, 3x3 mesh)

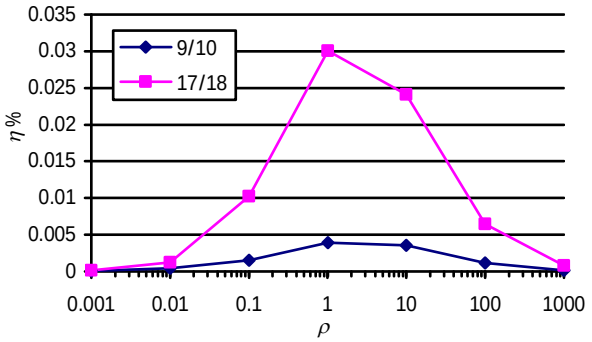

Figure 7: Local problem results (Reissner-Mindlin plate model, 4x4 mesh)

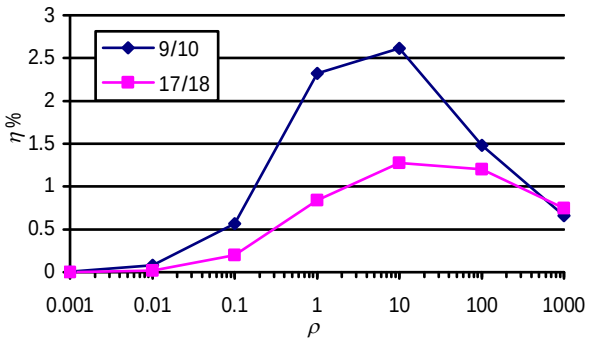

Figure 8: Local problem results (hierarchical plate model, 4x4 mesh)

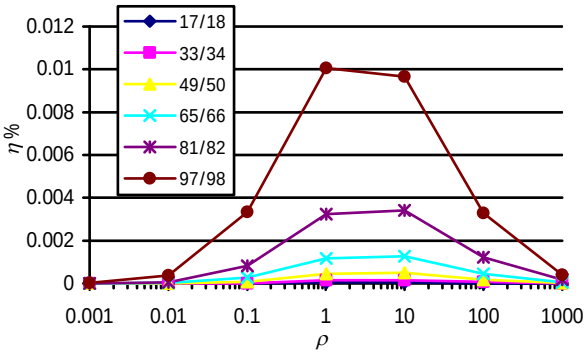

Figure 9: Local problem results (Reissner-Mindlin plate model, 8x8 mesh)

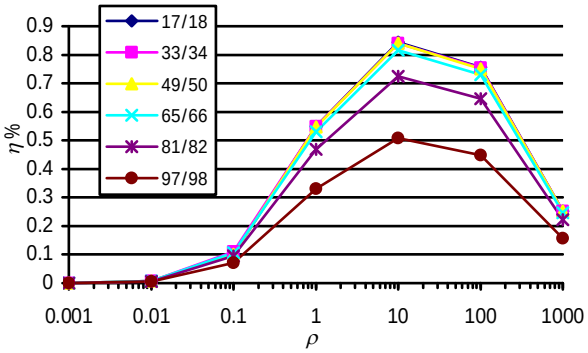

Figure 10: Local problem results (hierarchical plate model, 8x8 mesh)

Analyzing the obtained results one can observe the qualitative difference between the course of the curves obtained for the Reissner-Mindlin (Figs 5, 7 and 9) and hierarchical shell models (Figs 6, 8 and 10). Comparing the values of $\eta_{\%}$ corresponding to ρ values equal to 1 (arithmetic subdivision by 2) and 10 (exponential subdivision), one can observe the decrease for the former model and the increase for the latter one. This suggests the considerable influence of the boundary layer phenomenon on the solution results in the case of the hierarchical shell model and lack of such an influence in the case of the Reissner-Mindlin one.

Moreover, comparing the curves for three different meshes it can be noticed that for each of them, the results are in good qualitative agreement. This is true for both mechanical models of the plate. In spite of this, some local effects (the increase or decrease in $\eta_{\%}$ depends on the element pair location along the boundary) appear in the case of 8x8 mesh and the Reissner-Mindlin model.

In order to assess effectiveness of our tool we compare the above results with the control results obtained from the global problems in which the global mesh is divided as in the local four-element problems. The results are shown in Figs 11 to 16. They correspond to the local results presented in Figs 5-10, respectively.

Comparing the results of the global and local analyses one can see the qualitative agreement for both models and each of three regular meshes. The relation between values of $\eta_{\%}$ and ρ, corresponding to global results can be characterized exactly in the same way as for the local results. In most cases the qualitative agreement of the local and global results is quite astonishing.

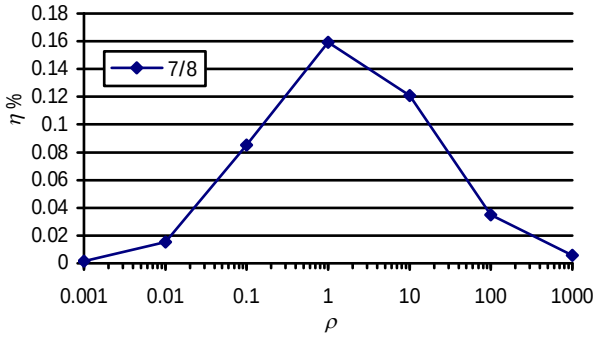

Figure 11: Global problem results (Reissner-Mindlin plate, 3x3 mesh)

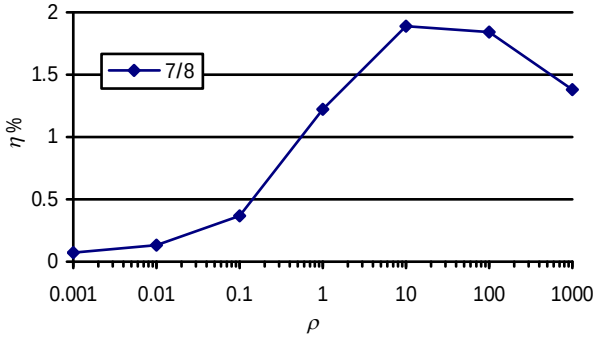

Figure 12: Global problem results (hierarchical plate model, 3x3 mesh)

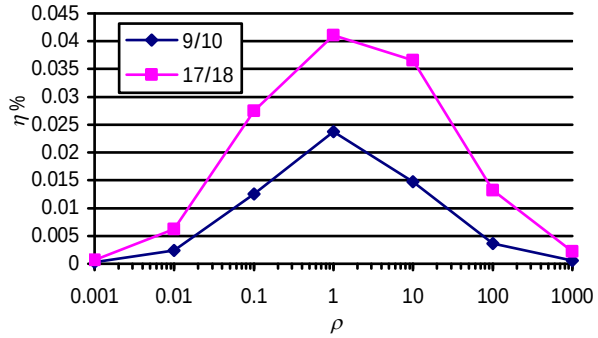

Figure 13: Global problem results (Reissner-Mindlin model of the plate, 4x4 mesh)

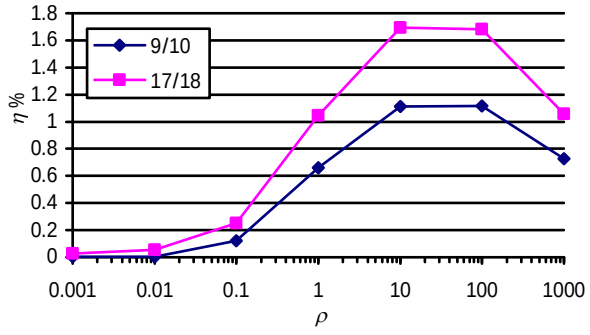

Figure 14: Global problem results 4x4 (hierarchical model of the plate, 4x4 mesh)

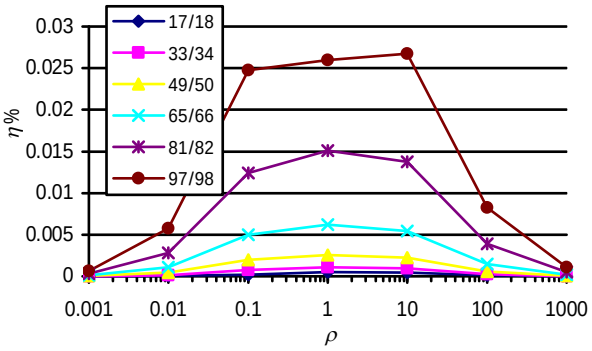

Figure 15: Global problem results (Reissner-Mindlin plate model, 8x8 mesh)

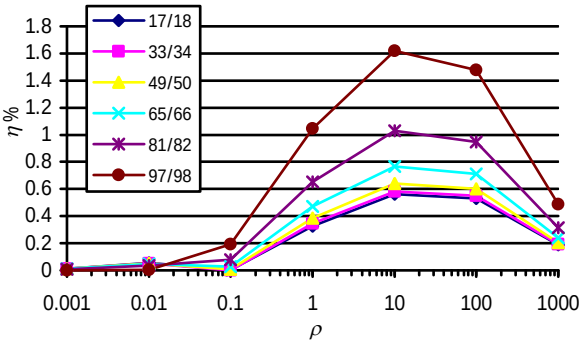

Figure 16: Global problem results (hierarchical plate model, 8x8 mesh)

Ending our discussion on the obtained results, we would like to address conditioning of the four-element problems for the extreme values of ρ. We have not observed any loss of solution stability for such values. This is confirmed by the 0 values of $\eta_{\%}$ for ρ=0.001 and ρ=1000. This can be interpreted as identity of the strain energies obtained from two- and four-element problems for which the conditioning problem does not exist and might have appeared, respectively. This observation was also confirmed with the equivalence of the number of common decimal digits in the values of the minimized strain energy and potential energy in four-element problems. For still lower or higher values of ρ one may checked the conditioning of the local problems with the standard method, applied by us previously in [9] to global problems.

4. Conclusions

In the case of the Reissner-Mindlin plate the results from the exponentially divided mesh are worse than those from the uniform mesh (compare Fig. 5, 7 and 9). In this case the boundary layer does not influence the results very much. This result is consistent with the theory.

In the case of the hierarchical shell model of the plate the situation is opposite (compare Fig. 6, 8 and 10). The influence of the boundary layer phenomena is visible.

The global results confirm the effectiveness of the proposed detection tool (compare Figs. 5 and 1, 7 and 13, 9 and 15, as well as 6 and 12, 8 and 14, 10 and 16).

It can be noticed that the detection of the boundary layer can be based on the results for only one chosen pair of elements from the boundary, provided that our choice is reasonable.

References

[1] Arnold D. N., R.S. Falk., Asymptotic analysis of the boundary layer for the Reissner-Mndlin plate model, *SIAM J. Math. Anal*., 27, pp.486-514, 1996.
[2] Dauge M., Gruais I., Rossle A., The influence of lateral boundary conditions on the asymptotics in the thin elastic plates, *SIAM J. Math. Anal*., 31, pp. 305-345, 2000.
[3] Cho J. R., Oden J. T., Locking and boundary layer in hierarchical models for thin elastic structures, *Comput. Methods Appl. Mech. Engrg*, 149, pp. 33-48, 1997.
[4] Schwab C., Suri M., Locking and boundary layer effects in the finite element approximation of Ressner-Mindlin plate model, *Proc. Symp. Appl. Math*., 48, pp. 367-371, 1994.
[5] Wempner G. *Mechanics of solids, with applications to thin bodies*. McGraw-Hill, New York, 1973.
[6] Zboiński, G., *Hierarchical Modelling and Finite Element Method for Adaptive Analysis of Complex Structures* (in Polish), Sci. Instal. of IFFM, No. 520/1479, IFFM, Polish Academy of Sciences, Gdańsk, 2001.
[7] Zboiński G., Ostachowicz W., Krawczuk M. *Modificationsof the adaptive procedur es for complex structures in the case of the improper solution limit, locking and boundary layers* (In Polish), Report no. 204/2000, IFFM, Polish Academy of Sciences, Gdańsk, 2000.
[8] Miazio, Ł., *The numerical tools for a posteriori detection of boundary layers and their effectiveness* (in Polish), Master's Thesis (supervisor G. Zboiński), Faculty of Technical Sciences, University of Warmia and Mazury, Olsztyn, 2008.
[9] Zboiński, G., 3D-Based *hp*-adaptive first order shell finite element for modelling and analysis of Complex Structures. Part 2. Application to structural analysis. *International Journal for Numerical Methods in Engineering*, 70, pp. 1546-1580, 2007.